Est. 1984

ORIENTAL JOURNAL OF CHEMISTRY
An International Open Free Access, Peer Reviewed Research Journal

www.orientjchem.org

ISSN: 0970-020 X
CODEN: OJCHEG
2017, Vol. 33, No. (1):
Pg. 249-257

Study on the Properties and Photoactivity of TiO_2 (nanorod)-SiO_2 Synthesized by Sonication Technique

SRI WAHYUNI[1,2], EKO SRI KUNARTI[1], RESPATI TRI SWASONO[1] and INDRIANA KARTINI[1]*

[1]Department of Chemistry, Faculty of Mathematics and Natural Sciences,
Universitas Gadjah Mada Sekip Utara Bulaksumur, Yogyakarta 55281, Indonesia
[2]Department of Chemistry, Faculty of Mathematics and Natural Sciences,
Universitas Negeri Semarang Jl.Taman Siswa, Sekaran, GunungPati, Semarang, 50221, Indonesia.
*Corresponding author E-mail: indriana@ugm.ac.id

http://dx.doi.org/10.13005/ojc/330129

(Received: October 13, 2016; Accepted: January 22, 2017)

ABSTRACT

A series of TiO_2 (nanorod)-SiO_2 nanocomposite (TS) with different mole ratios was prepared by sonication technique. Nanorod TiO_2 was prepared by solvothermal assisted by EDTA, while SiO_2 was prepared by sol-gel method. Various amount of SiO_2 powder was combined with nanorod TiO_2 to form TiO_2 (nanorod)-SiO_2 nanocomposite. Based on XRD and TEM results, the TiO_2 was rod-like anatase crystalline phase with the rod length of about 20-50 nm, while spherical SiO_2 was a large particle with a diameter of about 200 nm. The deposition of nanorod TiO_2 on the surface of spherical SiO_2 resulted in composites with slightly smaller crystallite size than that of the pristine nanorod TiO_2 of about 21-27 nm. The BET surface area of the TS composites was variable, of about 61.8–67.6 $m^2 g^{-1}$. The photoactivity of the composites was examined by measuring the zone inhibition of the composites to the growth of *E. coli* and *B. subtillis*, as a model of gram-negative and gram-positive bacteria, respectively. The composites have shown significant antimicrobial activity over both bacteria, which are slightly higher than that of pristine nanorod TiO_2.

Keywords: nanorod, TiO_2, SiO_2, nanocomposite, sonication.

INTRODUCTION

TiO_2 has been widely used as a photocatalyst in various applications from cleaning the environmental to generating electricity. These include applications in the air and water purification systems[1,2], products of self-cleaning surfaces[1,3],sterilization[1,3], hydrogen evolution[1,2], and photoelectrochemical conversion[4]. TiO_2 is considered an ideal semiconductor for photocatalysis because of its high stability, low cost and safety toward both humans and the environment[5]. The development of new materials, however, is strongly required to provide enhanced performances with respect to the photocatalytic properties and to find new uses for TiO_2 photocatalysis. TiO_2 or titania is also used in many applications like in pigments, ceramics, sun lotions, etc. Titania decomposes organic material

when illuminated with ultraviolet (UV) rays. This trait is utilised in the treatment of the waste material, air pollutant, drinking water, and in the development of self-cleaning surfaces[6-8].

Recently, titania supported on silica (SiO_2) have attracted much attention as advanced materials. A more uniform titania distribution was obtained by doping TiO_2 with SiO_2, ZrO_2, and other metal oxides[9-11]. The addition of SiO_2, or other oxides into anatase TiO_2 can improve the thermal stability and specific surface area[12-13]. An increase in the photocatalytic activity is an added advantage to the self-cleaning and antibacterial properties[14-15]. TiO_2 supported on silica was reported to exhibit a better photocatalytic performance than TiO_2 itself. This improved performance was believed due to the interaction between TiO_2 and SiO_2, and improved adsorption of the pollutant on the silica over pure TiO_2[16]. Various type of mixed oxide TiO_2-SiO_2 have been synthesised and applied to reduce organic dye pollutant[16]. TiO_2 and SiO_2 nanospheres were commonly used to prepare TiO_2-SiO_2 mixed oxide.

Recently, various types of TiO_2 such as nanorods, nanotubes, nanocrystals and mesoporous materials have been synthesized[17]. One-dimensional (1-D) TiO_2 nanostructures such as ellipsoidal nanoparticles[18], nanowires[19], and nanotubes[20], have been investigated extensively due to their special properties, which are attributed to dimensional anisotropy. Nanorod TiO_2 has been used to produce a superhydrophobic surface in a coating[19]. In 1-D nanostructured crystals of TiO_2, the space charge region is well constructed along the longitudinal direction of TiO_2 nanocrystal, meaning that photogenerated electrons can flow in the direction of the crystal length. Increased delocalization of electrons at 1-D nanostructured crystals can lead to a remarkable decrease in $e^H = e^-$ recombination probability[21].

In this study, the nanorod titania decorated on silica were synthesised by mixing silica sol and titania sol through sonication technique[16, 23]. Titania nanorod was prepared by solvothermal techniques[23]. On the other hand, SiO_2 nanoparticle was prepared by sol-gel methods[24]. If the surface of a larger particle is covered by a layer of fine particles, a core–shell system might be resulted[22]. The properties of nanorod TiO_2 decorated on SiO_2 at several compositions will be studied, including the surface area, crystallinity, crystallite size, and the effect of the composition of the mixed oxide on the photocatalytic activity. The photocatalytic performance of these materials was investigated by testing their ability to inhibit the growth of bacteria. *E. coli* was used to represent gram-negative bacteria and *B. subtillis* to represent gram-positive bacteria.

MATERIAL AND METHODS

All chemicals used in this experiment were of high purity and used as received. Titanium tetra-isopropoxide (TTIP, Sigma-Aldrich), anhydrous toluene (Mallinckrodt), ethylene diamine tetra-acetic acid disodium salt (Na_2EDTA, Sigma-Aldrich), tetraethyl orthosilicate (TEOS, Merck Germany) and ethanol (Merck Germany) were used as starting materials.

Synthesis of spherical SiO_2

The SiO_2 nanoparticles were synthesised using modified Stober process. The starting materials used for SiO_2 synthesis were TEOS, NH_3, ethanol, and H_2O with 9: 7: 7: 27 (v/v). TEOS and ethanol were mixed and stirred for 15 min. Then, NH_3 and H_2O were added dropwise slowly and carefully while sonication was performed for 2 h. All concentrations of the reactant were calculated based on final volume in the reaction mixture[24]. Sonication process took place in an Ultrasonic Homogenizer (Krisbow model 5510, 40 kHz).

Synthesis of nanorod TiO_2

Initially, 5 mmol of diethylene tetraacetic acid disodium salt (EDTA) complexing agent was added to 25 mL of millipore water and stirred until the dissolutions complete. The pH was maintained at around 8 by adding ammonia solution, and then 50 mL of toluene was slowly added and stirred for about 30 min. To this mixture, 5 ml of TTIP was added at a constant rate during the course of the reaction. The toluene to water ratio was set to 2:1, and the water to TTIP ratio was kept as 5:1. The solution turned into the slurry as a result of slow hydrolysis of TTIP in water. The final mixture was transferred into an autoclave (80% filling) sealed properly and heated

at a constant temperature of 180ºC for 3 h. The product was collected after centrifuge and washed repeatedly with millipore water and dried at 120ºC for 6 h[23].

Synthesis of TiO_2 (nanorod)-SiO_2

One gram of TiO_2 resulted from solvothermal method were dissolved in 50 mL ultrapure water, 1 mL HNO_3 0.1 M and 10 mL acetic acids were added in order to get the pH of 2 of the sol while sonicated for 10 min. The as-synthesized SiO_2 powder in the various mole percentages was dispersed in TiO_2 sol carefully. The mixture was dispersed in an ultrasonic bath for 30 min and kept for 24 h to form TiO_2deposited on SiO_2 sphere[16]. The suspension mixture then was filtered, dried, and calcined in air at 450°C for 3 h. The product was TiO_2-SiO_2 composite with 10%, 20%, and 30% mole content of $SiO_2$and named as TS-10, TS-20, and TS-30, respectively.

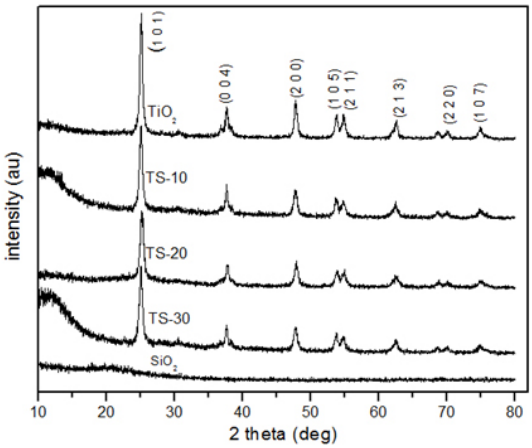

Fig. 1: XRD patterns of TiO_2, SiO_2, and different ratio of TS composite

Characterization

The crystal structure of powder was analysed by X-ray diffraction (XRD) using a Rigaku Miniflex 600, X-ray powder diffraction (Rigaku Corporation, Tokyo, Japan) with Ni-filtered Cu Ka (0.15418 nm) radiation at 45 kV and 20 mA. The crystallite size was calculated using the Scherer formula.

$$L=\frac{K\lambda}{\beta_{hkl}\cos\Theta}$$

where L is the average crystallite size in nm, K is a constant usually taken as 0.9, l is the wavelength of the X-ray radiation (using Cu Ka = 0.15418 nm), β_{hkl} is the line width at half-maximum height in radians, and θ is the diffracting angle[18,23]. The functional group of the compound was identified by Shimadzu FTIR-820 IPC. The Brunauer-Emmett-Teller (BET) surface area of TiO_2 and TiO_2-SiO_2 powders were determined using Surface Area Analyzer (Nova 3200e Quantachrome). The transmissions electron microscope (TEM) images were obtained using a JEOL JEM-1400 electron microscope to identify the morphology of TiO_2. Scanning Electron Microscopy (SEM) observations were carried out using a JEOL JSM-6510LA electron microscope.

Antimicrobial activity studies

The antimicrobial activity of the synthesised nanocomposites was investigated by well diffusion method against two bacterial strains, *Escherichia coli* (FN CC0051) as gram-negative bacteria, and *Bacillus subtilis* (ATCC 6633) as gram-positive

Table 1: The crystallite size and surface properties of TiO_2 and TS composite

Composite	Crystallite size(nm)*	BET surface area (m^2/g)	Pore volume (cm^3/g)	Pore diameter(nm)
SiO_2	-	12.159	0.038	11.85
TiO_2	30.60	63.988	0.344	21.52
TS-10	27.22	61.794	0.457	29.76
TS-20	20.95	67.561	0.410	24.24
TS-30	25.32	60.569	0.418	27.65

* calculated as average value of crystallite size from d_{101}, d_{200}, and d_{004}

bacteria. The obtained bacterial cultures were maintained on nutrient agar slants. The test bacterial suspensions (50 µL) containing 10^4 cells/mL were spread on nutrient agar plates. 50 µL nanomaterial (TiO_2) suspension or 50 mL nanocomposite (TiO_2-SiO_2) suspension (10 mg/mL) was added in the tested wells. The samples were initially incubated for 15 min at 4°C to allow diffusion and later illuminated with UV lamp (365 nm) for 40 min and then were incubated at 37°C for 12-18 h for the bacterial cultures[25].

RESULTS AND DISCUSSION

X-ray Diffraction

The powder XRD pattern of TiO_2 synthesized via Ti-EDTA chelated complex was presented in Fig. 1. The diffraction peaks are analogous to anatase crystal structure. For each sample, all peaks correspond to anatase phase at 2θ = 25.088, 37.6400, 47.7900, 53.7000, 54.8300, and 62.5570 (# 01-071-1168). It is found that the higher the percentage of SiO_2 the lower the intensity of the peaks. The peak associated with SiO_2 confirms an amorphous nature of silica. The increasing of SiO_2 particle in the formation of TiO_2-SiO_2 composites means the increasing of the amorphous particle into the composites, consequently the crystallinity will reduce as confirmed by less intense XRD peaks of the composites. From the data in Table 1, it appears that increasing the amount of SiO_2 in the composite also affect the crystallite size and surface area. This effect may be due to the SiO_2 limiting the agglomeration of nanorodTiO_2. Commonly, all crystallite size of the TS nanocomposite was not significantly different. Sirimahachai *et al.*[16] obtained a similar tendency about the influence of the amount of SiO_2 against the crystallinity and crystallite size of the composites.

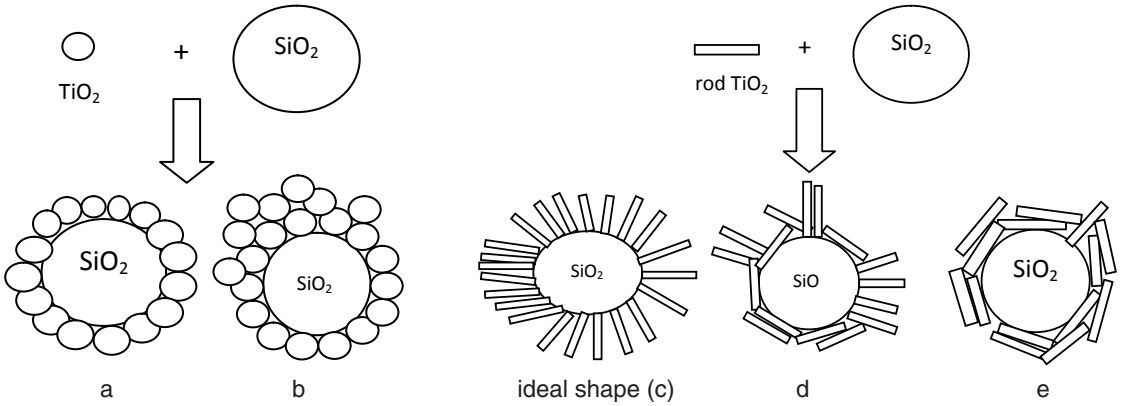

Fig. 2: Some composite model of TiO_2 deposited on SiO_2: a) and b) spherical TiO_2 coated SiO_2 c), d), and e) rod-shaped TiO_2 coated SiO_2

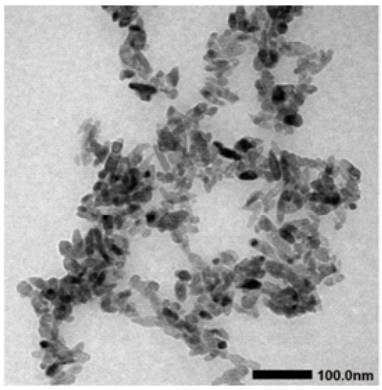

Fig. 3: TEM image of nanorods TiO_2

Fig. 2 is proposed to explain the arrested growth of nanorod TiO_2 by spherical SiO_2. It is assumed that the nanorod attachment on the spherical surface of silica is irregular (Fig. 2d). Thus, the crystallite sizes of the composites are variable.

Fig. 2a and 2b demonstrate the attachment model of the spherical TiO_2 on the surface of spherical SiO_2. These can affect the crystallite size of the resulted composites, resulting in small crystallites of TiO_2[16]. Spherical morphology of TiO_2 allows its deposition evenly over the surface of SiO_2. In another way, TiO_2 can be deposited in several layers, such

as forming an aggregation as suggested by Fig. 2b. The ideal model of nanorod TiO_2 attachment on the surface of silica is presented in Fig. 2(c), the rod-shaped TiO_2 are aligned vertically on the surface of SiO_2. Fig. 2d and 2e displayed other possible alignments of nanorod deposition on spherical surface. The nanorod may also attach vertically and horizontally on the surface of SiO_2.

TEM image

The TEM images of TiO_2 nanopowder (Fig. 3), shows the morphology of nanorods with the length size of about 50 nm. The TEM image endorses the formation of TiO_2 nanorods and their presence is quite consistent. To confirm the degree of orientation, the texture coefficient (TC) for (004) and (200) peaks of the oriented nanocomposite powder were determined and compared with the TC value of the standard TiO_2 powder[26]. TC of the synthesised TiO_2 was calculated from the relative intensity data in the XRD pattern (Fig. 1) and the PDF data file (# 01-071-1168). Deviation of TC values from unity implies preferred growth. A higher value of TC denotes preferred orientation of

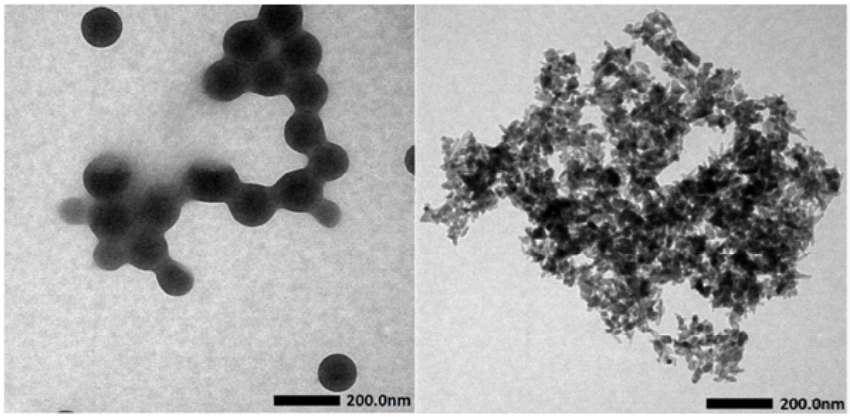

Fig. 4: TEM images for SiO_2 (left) and TiO_2(nanorod)-SiO_2(TS) (right)

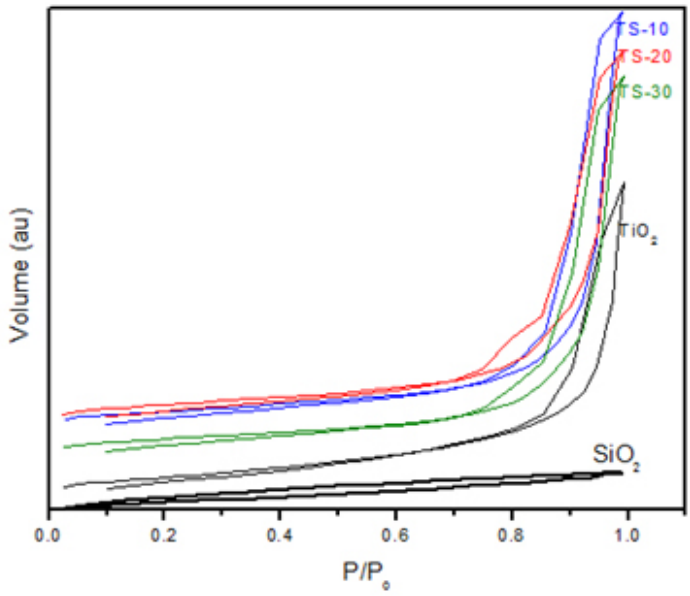

Fig. 5: N_2 adsorption-desorption isotherms of TiO_2, SiO_2 and composites of TiO_2-SiO_2 (TS)

grains[26]. The calculated TC (004) and (200) values of as-synthesized nanocomposite powder were 1.17 and 1.02 respectively. This oriented crystal growth obtained because of the act of EDTA as an orienting agent in the synthesis[23]. Christy *et al.* has been succeeding to synthesise nanorodsTiO_2 with a simple EDTA modifier[23].

The TEM images of SiO_2 and nanorod TiO_2 deposited on SiO_2 sphere were presented in Fig 4. From Fig. 4(left) the particle size of SiO_2 is about 100 nm. The spheres of silica are quite homogenous. Sirimahachai *et al.*[16] obtained spherical $SiO_2$with average size of about 350 nm. Wilhelm *et al.*[22] synthesised SiO_2 through Stober method at the various different size, from 150 nm until 590 nm. In this study, the particle size of SiO_2 was smaller than that of the SiO_2 reported by Sirimahachai *et al.*[16]. The spherical SiO_2 was then combined with nanorod TiO_2 with the length of about 50 nm. It is assumed that different size and morphology of the source of the composite produces rather a different shape and character of the composite.

BET Surface Area

The BET specific surface area (S_{BET}) was calculated by using the standard BET method on the basis of the adsorption data[28]. The nitrogen adsorption-desorption isotherms of TiO_2, SiO_2, and TiO_2-SiO_2 (TS) material are shown in Fig. 5. Their different appearances suggest the modifications of the porosity characteristics when the mixed oxides form a new network. The isotherm curve for SiO_2, shows a type IV isotherm with a broad type H4 hysteresis loop, in the middle range of relatively pressure. This could be associated with the presence of narrow slit pores[29]. For TiO_2 and TS material, type IV isotherms with type H1 hysteresis loop in relatively high pressure are observed. It can be associated with a porous material consisting of well-defined cylindrical-like pore channels[29].This supports the synthesis design that the nanorod TiO_2 covering the surface of the spherical SiO_2.

Sirimahachai *et al.*[16] reported the relatively significant change of surface area against the increasing of SiO_2, due to the sphere morphology of both SiO_2 and TiO_2. In this research, the TiO_2 deposited on SiO_2 was rod-shaped. The surface areas of the composites are just slightly changed against the SiO_2 content. It is predicted that nanorod morphology of TiO_2 will provide steric hindrance to covering the SiO_2 particle completely as depicted in Fig. 2d-e.Therefore, the surface areas of the composites are almost the same.

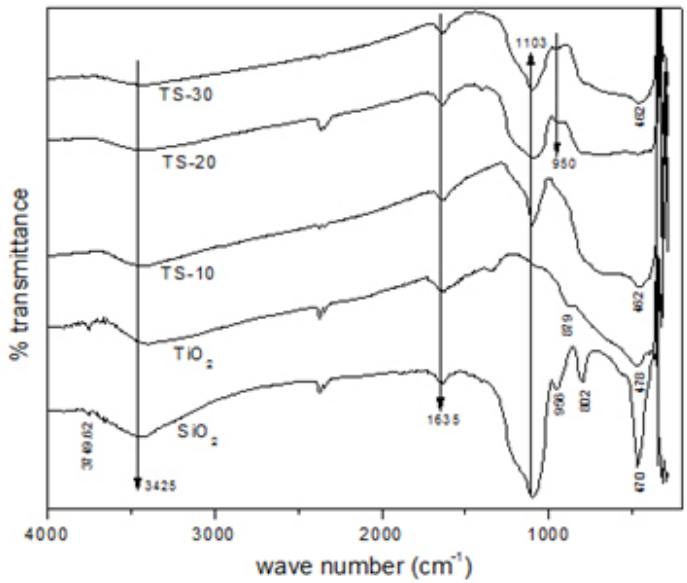

Fig. 6: The FTIR spectra of TiO_2, SiO_2 and composites of TiO_2-SiO_2 (TS)

FT-IR spectra

The FT-IR spectra of nanorod TiO_2 and TS composite with a various mole ratio of SiO_2 are presented in Figure 6. IR spectra of pure silica were also taken for comparison. The absorption bands at around 3426 and 1635 cm^{-1} observed in all spectra are attributed to the stretching mode of water and hydroxyl group[14]. The peak around 802 cm^{-1} and 1103 cm^{-1} are ascribed to the symmetric vibration of Si–O–Si and the asymmetric stretching vibration of Si–O–Si, respectively[16]. The peak at 950 cm^{-1} corresponding to the vibration of Si–O–Ti confirmed the formation of Si–O–Ti inorganic network between SiO_2 and TiO_2 in TS-20 and TS-30 samples[30]. In TS-10, the amount of silica is too low for the formation of Si–O–Ti network, hence a peak for Si–O–Ti could not be observed. It is also clear that composites spectra are a combination of the pure SiO_2 spectra and pure TiO_2 spectra[14].

SEM image

For further characterization of the nanorod TiO_2 deposited on SiO_2, SEM studies were done. Figure 7 shows SEM images of the SiO_2 and TiO_2 deposited on SiO_2 (TS) particles. The image of SiO_2 illustrates that the particles are spherical and have a smooth surface. After the deposition process, SEM image shows that the coated silica is still spherical, but the surface of the particles is not smooth anymore. This can be ascribed to the presence of nanorod titania deposited on the surface of spherical silica. Similar result was carried out by heterogenic coagulation method to depositing spherical TiO_2 on the surface of SiO_2[23, 31]. It can be concluded that the nanorod attachment may follow Fig. 2e.

Antimicrobial activity

Antimicrobial activity of nanorod$TiO_2$and TiO_2 (nanorod)-SiO_2(TS) composites were

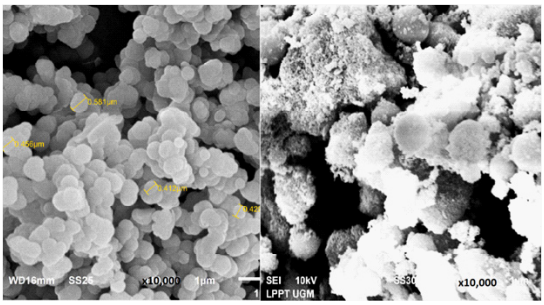

Fig. 7: SEM images for SiO_2(left) and TS-20 (right)

Table 2: Mean Diameter of Inhibitory Zone (mm) of TiO_2 and TiO_2-SiO_2 against Bacterial Strains *Bacilus subtillis* and *Escherichia coli*

Composite	*B subtillis*	*E coli*
SiO_2	-	-
TiO_2	12.0	17
TS-10	17.0	19
TS-20	19.0	23
TS-30	17.0	18

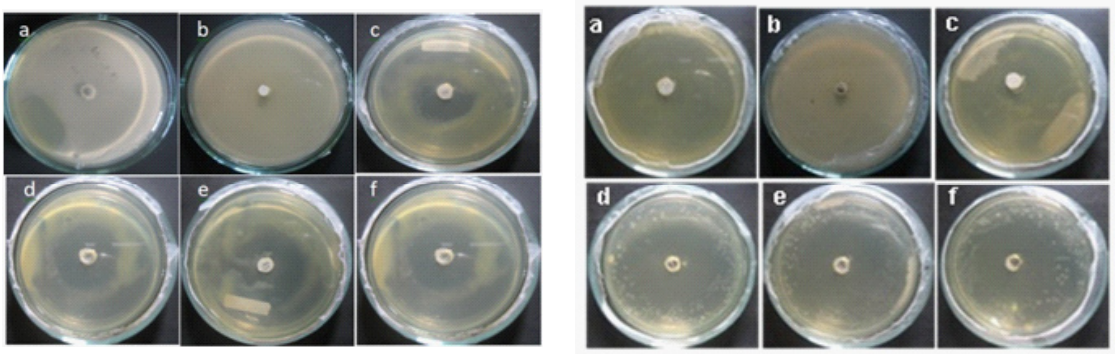

Fig. 8: Zone inhibition of TiO_2 and TiO_2/SiO_2 against *B subtilis* (I) and *E coli* (II) a. Blank, b. SiO_2, c. TiO_2, d. TS-10, e. TS-20, f. TS-30

investigated by well diffusion method against *E. coli* and *B. subtillis*. All tests and inoculation on each plate were run in duplicates. The results then were inspected visually (Fig. 8) and zone inhibition values were recorded (Table 2). Figure 8 (I) and (II) shows inhibition zone for *B. subtillis* and *E. coli* respectively. TS-20 composite gives the largest inhibition zone for both *B. subtillis* and *E. coli.* This result may have a relationship with the BET surface area, which shows the largest area for this composite. Sirimahachai *et al.*[32] investigated the performance of various TiO_2 to inhibit bacterial growth and obtained the best result for the TiO_2 nanoparticles with the largest surface area (320.1 $m^2 g^{-1}$). In this study, TS-20 composite inhibits the growth of the bacteria at the same concentration (50 mg/mL) but with the smaller surface area (67.561 $m^2 g^{-1}$). The same result was also obtained by Piskin *et al.*[25] which investigated the TiO_2 sol synthesised by sonication technique.

All samples also demonstrate higher inhibition toward gram-negative bacteria compare to the gram-positive bacteria. The gram-positive bacteria, *B. subtillis*, have a relatively thick wall composed of many layers of peptidoglycan polymer and only one layer of membrane. The gram-negative bacteria (*E. coli*) have only a thin layer of peptidoglycan and a more complex cell wall with two cell membranes, an outer membrane, and a plasma membrane.

CONCLUSIONS

It is concluded that the major phase of the nanorod TiO_2 particle and TiO_2-SiO_2 composites are the anatase crystalline phase. The presence of silica has retarded the grain growth of nanorod titania so considerably, that the particle size of the composite is slightly smaller than that of pristine TiO_2.The SEM image of the composite structure confirms the attachment of nanorod titania on the surface of spherical silica. The sonication technique provides a facile technique to produce a composite of titania–silica with a good crystallinity and surface area from TiO_2 and SiO_2 sols as the precursors. TiO_2 (nanorod)-SiO_2composites have also shown good antimicrobial performance at a small surface area, that might be contributed by the nanorod structure. Study on hydrophobicity properties induced by the nanorod TiO_2 over the SiO_2 is underway.

ACKNOWLEDGEMENTS

We are thankful to the Laboratory of Microbiology, Department of Biology UNNES and LPPT UGM for providing all facilities to direct this work. SW is grateful to the Directorate General of Higher Education for providing a doctoral scholarship.

REFERENCES

1. Nakata, K. and Fujishima, A. *J. Photochem. Photobiol., C,***2012**; *13*, 169–189.
2. Arora, A. K., Jaswal, V. S., Singh, K. and Singh, R., *Orient. J. Chem.*, **2016**; *32*(4),2035-2042.
3. Kartini, I., Santosa, S. J., Febriyanti, E., Nugroho, O. R., Yu, H. and Wang, L., *J. Nanopart. Res.*, **2014**; *16*, 2514
4. Kartini, I., Menzies, D., Blake, D., da Costa, J. C. D, Meredith, P., Riches, J. D. and Lu, G. Q., *J. Mater. Chem.*, **2004**; *14*, 2917–29212.
5. Gupta, S. M. and Tripathi, M. *Chin. Sci. Bull.*, **2011**; *56*(16), 1639–1657.
6. Dalton, J.S., Janes, P.A., Jones, N.G., Nicholson, J.A. Hallam, K.R. and Allen, G.C., *Environ. Pollut.*, **2002**; *120*, 415-422.
7. Liu,Y., Wang, X., Yang, F. and Yang, X., *Micropor. Mesopor. Mater.*, **2008**; *114*, 431–439.
8. Aprilita, N. H., Kartini, I. and Ratnaningtyas, S. H., *Indones. J. Chem,.***2008**, *8*, 200-206.
9. Uchiyama, H., Suzuki, K.,Oaki, Y.,and Imai, H., *Mater. Sci. Eng. B*, **2005**; *123*, 248–251.
10. Reddy, B. M., Reddy, G. K., Rao, K. N., Ganesh, I., and Ferreira, J. M. F., *J. Mater. Sci.,***2009**; *44*, 4874–4882.
11. Fujishima, A., Rao, T. N., and Tryk, D. A., *J. Photochem. Photobiol., C,* **2000**; *1*, 1-21.
12. Rahmani, E., Ahmadpour, A., and Zebarjad,

M., *Chem. Eng. J.,***2011**; *174*, 709-713.
13. Castillo, R., Koch, B., Ruiz, P., and Delmon, B., *J. Mater. Chem.*,**1994**; *4*, 903-908.
14. Smitha, V. S., Manjumol, K. A., Baiju, K. V., Ghosh, S., Perumal, P. and Warrier, K. G. K., *J. Sol-Gel Sci. Technol.,***2010**; *54*, 203-211.
15. Allen, N. S., Edge,M., Verran,J., Stratton,J., Maltby, J., and Bygott, C., *Polym. Degrad. Stab.*, **2008**; *93*,1632-1646.
16. Sirimahachai, U.,Ndiege, N., Chandrasekharan, R.,Wongnawa, S., and Shannon, M. A., *J. Sol-Gel Sci. Technol.*, **2010**; *56*, 53-60.
17. Yeung, K.L., Leung, W.K., Yao, N. and Cao, S., *Catal. Today*, **2009**; *143*, 218-224.
18. Kang, S.H., Choi, S.H., Kang, M.S., Kim, J.Y., Kim, H.S., Hyeon, T., and Sung, Y.E., *Adv. Mater.*, **2008**; *20*, 54-58.
19. Zhang, X., Guo, Y., Zhang, Z., and Zhang, P., *Appl. Surf. Sci.*, **2013**; *284*, 319–323.
20. Joo, J., Kwon, S.G., Yu, T., Cho,M., Lee, J., and Yoon, J., *J. Phys. Chem. B*, **2005**; *109*, 15297-15302.
21. Yun, H.J., Lee, H., Joo, J.B., Kim, W., Yi, J., and Yun, J., *J. Phys. Chem. C.,* **2009**; *113*, 3050-3055.
22. Wilhelm, P. and Stephan, D., *J. Coll Inter. Sci.*, **2006**; *293*, 88-92.
23. Christy, P.D., Melikechi, N., Nirmala Jothi, N.S., Baby Suganthi, A.R. and Sagayaraj, P. *J. Nanopart. Res.*, **2010**; *12*, 2875-2882.
24. Rahman, I.A.,Vejayakumaran, P., Sipaut, C.S., Ismail, J.,Bakar, M.A., Adnan, R., and Chee, C.K., *Colloids Surf. A.*, **2007**; *94***,** 102-110.
25. Piºkin, S., Palantöken, A., and Yýlmaz, M.S., *Proceedings of International Conference on Emerging Trends in Engineering and Technology (ICETET)*, Patong Beach, Phuket, Thailand,**2013**; 91-94.
26. Sadhu, S, and Poddar, P., *J. Phys. Chem. C*, **2014**; *118*, 19363–19373.
27. Polleux, J., Pinna, N., Antonietti, M., and Niederberger, M. *Adv. Mater.*, **2004**;*16*(5), 436–439.
28. Brunauer, S. Emmett, P.H. and Teller, E. *J. Am. Chem. Soc.*, **1938**; *60*, 309-319.
29. Carja, G., Nakamura, R., Aida, T. and Niiyama, H., *Micropor. Mesopor. Mater.*, **2001**; *47*, 275-284.
30. Cheng, P., Zheng, M., Jin, Y., Huang, Q., and Gu, M., *Mater.Lett.,* **2003**; *57*(20), 2989–2994.
31. Wilhelm, P. and Stephan, D. *J. Photochem. Photobiol., A*, **2006**; *185***,** 19–25.
32. Sirimahachai, U., Phongpaichit, S., and Wongnawa, S. *Songklanakarin J. Sci. Technol.*, **2009**; *31***,** 517-525.